IBRO Reports 7 (2019) 42–51

Contents lists available at ScienceDirect

IBRO Reports

journal homepage: www.elsevier.com/locate/ibror

Research Paper

Follow-up study of subventricular zone progenitors with multiple rounds of cell division during sulcogyrogenesis in the ferret cerebral cortex

Kazuhiko Sawada*

Department of Nutrition, Faculty of Medical and Health Sciences, Tsukuba International University, Tsuchiura, Ibaraki 300-0051, Japan

ARTICLE INFO

Keywords:
Outer subventricular zone
Basal radial glia
Gyrification
Carnivores
Evolutionary expansion

ABSTRACT

The subventricular zone (SVZ) of the developing cerebral cortex appears transiently during cortical neurogenesis and is known as the second proliferative zone that contains intermediate progenitor cells and self-renewable neuronal stem cells—the so-called basal radial glia (bRG). The present study attempted to track the differentiation and migration dynamics of SVZ progenitors undergoing multiple cell divisions at the late stage of neurogenesis in a course of sulcogyrogenesis in the ferret, a gyrencephalic mammal. Ferret pups were given a 5-ethynyl-2′-deoxyuridine (EdU) injection on postnatal day (PD) 5 followed by a 5-bromo-2′-deoxyuridine (BrdU) injection on PD 7. The 48 h interval between EdU and BrdU injections covered the minimum times for the first and second S-phase of self-renewing bRG. Two h after BrdU injection, EdU/BrdU-double labeled cells were found in the inner or outer SVZ (iSVZ and oSVZ), more than 80% of which were Sox2-positive. Furthermore, 95.8% of EdU/BrdU-double labeled Sox2-positive progenitors in the iSVZ and 84.2% in the oSVZ were also Pax6-positive, defining these progenitors as bRG. On PD 20, all EdU/BrdU-double labeled cells were NeuN-immunopositive, and more than 60% of these were parvalbumin-immunopositive. EdU/BrdU-double labeled neurons were distributed densely in the superficial portion of the outer cortical stratum. Cluster analysis divided the gyral and sulcal regions into higher and lower density groups, respectively, based on the diversity of the cortical density of EdU/BrdU-double labeled neurons. The higher density group included the gyral and sulcal regions of the prefrontal, parietooccipital and/or cingulate cortex, corresponding to cortical regions associated with evolutionary expansion. Although a limited population of neurons within a narrow time window of cortical neurogenesis was tracked, the present findings suggest that neurons derived from bRG at the late stage of neurogenesis express parvalbumin during corticohistogenesis. Due to the diversity of sulcogyral distributions, neurons derived from bRG may be implicated in evolutionary cortical expansion.

1. Introduction

The subventricular zone in the developing cerebral cortex appears transiently during cortical neurogenesis and is known as the second proliferative zone that contains intermediate progenitor cells (IPC) and self-renewable neuronal stem cells—the so-called basal radial glia (bRG; also known as the outer radial glia (oRG) or transient radial glia (tRG)) (Lui et al., 2011). The bRG is found either in the inner or outer subventricular zone (iSVZ and oSVZ) of the developing cerebral cortex in many mammalian species including humans (Hansen et al., 2010; Fietz et al., 2010), rhesus macaques (Martínez-Cerdeño, et al., 2012), marmosets (Kelava et al., 2012), cats (Reillo et al., 2011), ferrets (Fietz et al., 2010; Reillo et al., 2011; Martínez-Cerdeño et al., 2012), rats (Martínez-Cerdeño et al., 2012), and mice (Reillo et al., 2011; Shitamukai et al., 2011; Wang et al., 2011), and is a major source of neurons in the massively-expanded mammalian cortex (Lewitus et al., 2013). Nonaka-Kinoshita et al. (2013) described the bRG as one of the factors involved in the evolutionary expansion of the cerebral cortex. Notably, the bRG is abundant in the oSVZ of gyrencephalic primates and carnivores, but less abundant in lissencephalic rodents (Reillo et al., 2011). In a previous study, the oSVZ was found to expand prior to cortical folding in the marmoset cerebral cortex (Sawada et al., 2014). Enhanced cortical folding can be induced by increasing the progenitor pool containing bRG by genetic manipulation of novel nuclear antigens, such as Tmp1 and BAF170 (Stahl et al., 2013; Tuoc et al., 2013), and sonic hedgehog (shh) signaling (Wang et al., 2016) in mice as well as FGF8 and FGR receptors (Masuda et al., 2015; Matsumoto et al., 2017) and human-specific *ARHGAP11B* (Kalebic et al., 2018) in ferrets. The contribution of oSVZ progenitors, particularly bRG, to macroscale morphogenesis of the cerebral cortex has been previously discussed

* Corresponding author.
E-mail address: k-sawada@tius.ac.jp.

https://doi.org/10.1016/j.ibror.2019.07.1720
Received 15 March 2019; Accepted 27 July 2019

(Borrell, 2018). The current investigation attempted to track the differentiation and migration dynamics of SVZ progenitors with multiple cell divisions at the late stage of neurogenesis in a course of sulcogyrogenesis in a gyrencephalic mammal, namely the ferret. Ferrets have advantageous characteristics for investigating gyrification mechanisms because of a prolific animal experiencing sulcogyrogenesis after birth (Sawada and Watanabe, 2012; Sawada et al., 2015; Sawada and Aoki, 2017; Kroenke and Bayly, 2018). The present study focused on the fact that the cell cycle length differs between bRG and IPC in the developing ferret cortex (Turrero García et al., 2016). Two thymidine analogues, namely 5-ethynyl-2′-deoxyuridine (EdU) and 5-bromo-2′-deoxyuridine (BrdU), were injected into ferret pups after a 48 h interval, which covered the minimum times for the first and second S-phase of the self-renewing bRG in ferrets.

2. Materials and methods

2.1. Animals

Five ferret pups, delivered by three different ferret dams, were obtained at postnatal day (PD) 5 from SLC (Hamamatsu, Japan). The pups were reared with lactating mothers (2 or 3 pups/mother) and housed in stainless-steel cages (80 cm × 50 cm × 35 cm) at 21.5 ± 2.5 °C under 12 h artificial illumination in the Faculty of Animal Breeding, Nakaizu Laboratory, SLC. All lactating mothers were given a pellet diet (High Density Ferret Diet 5L14, PMI Feeds, Inc., St. Louis, Mo.) and tap water *ad libitum*.

All ferret pups received an intraperitoneal injection of 30 μg/g body weight of EdU (Sigma-Aldrich, St. Louis, MO) on PD 5 and an intraperitoneal injection of 30 μg/g body weight of BrdU (Sigma-Aldrich) 48 h after EdU injection. Pups were then divided into two groups. The first group consisted of 2 ferret pups perfused with 10 mM phosphate buffered saline, pH 7.4 (PBS), followed by 4% paraformaldehyde in PBS (PFA solution), under deep anesthesia with an intraperitoneal injection of 400 μg/g body weight of chloral hydrate (Wako Pure Chemical Industries, Ltd. Osaka, Japan) 2 h after BrdU injection. The second group consisted of 3 ferret pups perfused with the same reagents on PD 20 following the same procedure.

All procedures were performed in accordance with the guidelines of the National Institutes of Health (NIH) for the Care and Use of Laboratory Animals and approved by the Institutional Animal Care and Use Committee of Tsukuba International University. All procedures attempted to minimize the number and suffering of animals used.

2.2. Immunohistochemical procedures

The right and left cerebral hemispheres were separated at the longitudinal cerebral fissure and immersed in 30% sucrose in PBS overnight. Cerebral hemispheres were embedded in optimal cutting temperature compound and sectioned serially along the coronal plane at 100 μm using a Retratome (REM-700; Yamato Koki Industrial Co. Ltd. Asaka, Japan) with a refrigeration unit (Electro Freeze MC-802A, Yamato Koki Industrial). Sections were serially collected into vials containing PFA solution. Coronal sections at levels of the anterior commissure were selected from the cerebral hemisphere of seven-day-old ferret pups. These sections included a largely-expanded oSVZ. Four sets of coronal sections at the levels indicated in Supplemental Fig. 1 were selected from the cerebral hemispheres of 20-day-old ferret pups. These sections included the major primary sulci and gyri. To select sections containing identical cortical regions within sulci and gyri, the cortical laminar structures in each region were referred to (Horiuchi-Hirose and Sawada, 2016).

All immunohistochemical procedures were performed on floating sections. To allow comparison of immunostaining results, all sections were processed with identical staining conditions. The same sets of solutions were used for the respective times and temperatures of incubation for antigen retrieval treatment, including the primary and secondary antibodies, time, temperature, and number of PBS washings.

All sections were treated with Antigen Retrieval Reagent UNIVERSAL (R&D system, Minneapolis, MN) for 30 min in a 90 °C water bath and then cooled at 4 °C for 30 min. The sections were subsequently treated with 4 N HCl at 37 °C for 30 min, followed by neutralization with 0.1 N sodium borate buffer, pH 8.5, at 37 °C for 30 min. After incubation with PBS containing 0.1% Triton-X 100 (Sigma Aldrich) at 37 °C for 1 h, sections were reacted with a Click-iT reaction cocktail containing Alexa Fluor 488 (Click-iT EdU Alexa Fluor 488 Imaging Kit; Thermo Fisher Scientific, Waltham, MA, USA) for detecting EdU at 37 °C for 1 h. After rinsing with PBS, sections were reacted with primary antibodies (see below) in PBS containing 0.1% Triton-X 100 and 10% normal horse serum (Vector Labs. Inc. Burlingame, CA) at 4 °C overnight. Primary antibodies included a rat antibody to BrdU (1:1,000; ab6326, Abcam, Cambridge, UK), a goat antibody to Sox2 (1:1,000; AF2018, R&D Systems, Minneapolis, MN, USA), rabbit antibodies to NeuN (1:1,000; ABN78; Millipore), cleaved caspase 3 (cCP3) (1:500; GTX22302, GeneTex Inc. Irvine, CA) and Olig2 (1:1,000; IBL, Gunma, Japan), and mouse antibodies to Pax6 (1:500, ab78545, Abcam), GFAP (1:1,000, G 3893, Sigma-Aldrich), and parvalbumin (PV) (1:500; PV235, Swant, Switzerland). These primary antibodies were produced by highly specific immunostaining in ferret tissues (Poluch et al., 2008; Reillo et al., 2011; Kelava et al., 2012; Martínez-Cerdeño et al., 2012; Di Curzio et al., 2013; Gertz et al., 2014; Kawasaki et al., 2013; Saliu et al., 2014; Masuda et al., 2015). After incubation, the sections were reacted with appropriate secondary antibodies (see below) at 37 °C for 3 h, followed by incubation with streptavidin conjugated to AMCA (1:100; SA-5008, Vector Labs) or streptavidin conjugated to Alexa 555 (1:500, S21381, Thermo Fisher Scientific) at 37 °C for 1 h when using biotinylated secondary antibodies. Secondary antibodies included Alexa 350 goat anti-rat IgG (1:500; A-21093, Thermo Fisher Scientific), Alexa 488 donkey anti-mouse IgG (1:500; A-21202, Thermo Fisher Scientific), Alexa 555 donkey anti-rabbit IgG (1:500; A-31572, Thermo Fisher Scientific), Alexa 555 donkey anti-mouse IgG (1:500; A-31570, Thermo Fisher Scientific), Alexa 555 donkey anti-goat IgG (1:500; A-21432, Thermo Fisher Scientific), Alexa 647 chicken anti-rat IgG (1:500; A-21472, Thermo Fisher Scientific), and biotinylated donkey anti-rabbit IgG (1:200; A16027, Thermo Fisher Scientific). After washing with PBS, the sections were mounted on slides and coverslipped with glycerin.

2.3. Evaluation of immunolabeled and/or thymidine analogue-labeled cell density

Images of immunolabeled and/or thymidine analogue-labeled sections were acquired with a 20× objective by serial digital sectioning (section plane thickness = 1 μm; number of sections = 10) using an Axioimager. M2 ApoTome.2 microscope equipped with an AxioCam MRm camera (Zeiss, Gottingen, Germany) using ZEN 2.3 (blue edition) software (Zeiss). A set of sectional images 4 μm apart at the Z-direction (the third and seventh Z-axis slices of the acquired images) were selected as lookup and reference images, respectively, to evaluate the immunolabeled and/or thymidine analogue-labeled cell density by systematic random sampling. Immunolabeled and/or thymidine analogue-labeled cell density was estimated by the disector method, which is based primarily on a procedure by Fukui and Bedi (2000). The counting frames consisted of 3 or 6 square boxes (box size = 80 μm × 80 μm). On PD 7 sections, the counting frames were superimposed randomly on the iSVZ and oSVZ of both lookup and reference images at the same positions perpendicular to the ventricular surface. On PD 20 sections, the counting frames were superimposed randomly on the superficial portion of the outer stratum (layer II adjacent to layer I), outer stratum (layers II and/or III underlying the superficial portion), and inner strata (layers IV to VI) of gyral crowns and sulcal floors. A total of 3 or 6 pairs of regions of interest (ROIs) were selected systematically within the counting frames (Supplemental

Fig. 2 A). Immunolabelled or thymidine analogue-labeled cells within the ROI were counted using the “forbidden line” rule (Gundersen, 1977) (Supplemental Fig. 2B), and their density was estimated using the stereological formula [Nvn = Qn^{-}/(a*t)] (Sterio, 1984) where Qn^{-} = the number of immunolabeled and/or thymidine analogue-labeled in the lookup images, but not the reference images (Supplemental Fig. 2C); a = 3–6 (number of total areas examined in the lookup images); and t = 4 μm (distance between the lookup and reference images). The proportions of immunolabeled or thymidine analogue-labeled cells positive for the various markers were calculated using the summed data counted within all ROIs.

2.4. Statistical analysis

All measurements of the left and right hemispheres were separately quantified. Quantification was followed by paired sampled *t*-tests to assess no significant left/right differences, and data on each side were considered to be $n = 1$. Due to the small sample size, a non-parametric procedure was used for statistical evaluation. The Friedman test followed by non-parametric type Scheffe’s test were performed to assess differences in the density of immunolabeled and/or thymidine analogue-labeled cells among gyral or sulcal regions.

Cluster analysis was carried out using the Euclidean distance and Ward's method. Gyral and sulcal regions were divided into two groups based on the diversity of EdU/BrdU-double labeled cell density among cortical strata of the sulcal and gyral regions, respectively.

Regional differences in the proportions of immunolabeled or thymidine analogue-labeled cells positive for the markers were statistically evaluated by the Chi-square test for all comparisons among the gyral and sulcal regions examined. The total number of immunolabeled or thymidine analogue-labeled cells counted was defined as “n” for the Chi-square test.

3. Results

3.1. EdU/BrdU-double Labeled Cells in the iSVZ and oSVZ of seven-day-old ferrets

EdU/BrdU-double labeled cells were immunohistochemically characterized in the premature cortex of ferret pups on PD 7 at 2 h after BrdU injection. Identification of premature cortical layers was performed primarily according to Martınez-Cerdeno et al. (2012). Sox2-positive and Pax6-positive progenitors were distributed abundantly through the iSVZ to oSVZ on PD 7 (Fig. 1A, B), and a significantly greater density was marked in the iSVZ relative to the oSVZ (Table 1). Pax6 immunostaining was present in Sox2-positive progenitors (Fig. 1C, D) and the proportion was 34.8% in the oSVZ, which was significantly higher than 22.1% in the iSVZ ($P < 0.01$) (Table 2). Since Pax6 is known as a marker for bRG across species (Kelava et al., 2012; Reillo and Borrell, 2012; Martínez-Cerdeño et al., 2012), Sox2-positive/Pax6-positive progenitors were defined as the bRG. However, Olig2-positive cells were also found in the premature cortex (Fig. 2). Less than 30% of Sox2-positive progenitors were Olig2-positive, and the proportion was significantly greater in the oSVZ (28.6%) than in the iSVZ (12.4%; $P < 0.01$) (Table 2).

EdU/BrdU-double labeled cells were found in the ferret premature cortex on PD 7 (Figs. 1,2). Although EdU-single and BrdU-single labeled cells were significantly denser in the iSVZ than the oSVZ, no statistically significant difference in EdU/BrdU-double labeled cell density was found between these two zones (Table 1), suggesting a prominent presence of EdU/BrdU-double labeled cells in the oSVZ. Sox2 immunostaining appeared in EdU/BrdU-double labeled cells at 85.3% in the iSVZ and 90.6% in the oSVZ (Table 3). Notably, 95.8% and 84.2% of EdU/BrdU-double labeled Sox2-positive progenitors were Pax6-positive in the iSVZ and oSVZ, respectively (Table 3), although EdU/BrdU-double labeling was observed in Sox2-positive/Pax6-positive progenitors at only 14.3% and 13.3% in the iSVZ and oSVZ, respectively (Table 4). There was a 48 h interval between EdU injection (9:00–9:30 AM on PD 5) and BrdU injection (9:00–9:30 AM on PD 7). While the cell cycle duration varies among stem cell/progenitor subpopulations, the total cell cycle length and duration of S-phase are 68.7 and 22.6 h, respectively, in the bRG of the developing ferret cortex (Turrero García et al., 2016). The design of EdU and BrdU injections in the present paper labeled a certain number of bRGs experiencing multiple cell divisions on PDs 5 and 7, albeit the proportions were low. Furthermore, 30.0% and 47.4% of Sox2-positive progenitors with EdU/BrdU-dual labeling were Olig2-positive in the iSVZ and oSVZ, respectively (Table 3). EdU/BrdU-double labeled bRG might include Olig2 expressing subtypes, which were not prominent subpopulations.

Double immunofluorescence staining for Sox2 and cCP3 with EdU and BrdU labeling was carried out to further clarify whether EdU/BrdU-double labeled cells were apoptotic in the premature cortex. As shown in Figs. 3A and 3B, cCP3-positive cells were present in both the iSVZ and oSVZ of the premature cortex of PD 7 ferrets. cCP3 immunostaining appeared in 15.2% and 12.1% of Sox2-positive progenitors in the iSVZ and oSVZ, respectively (Table 2). Furthermore, cCP3 immunostaining was seen in 20% of EdU/BrdU-double labeled Sox2-positive progenitors in the oSVZ, which was significantly lower than the 60.0% seen in the iSVZ ($P < 0.05$) (Table 3). Thus, Sox2-positive progenitors experiencing multiple cell divisions at PDs 5 and 7 were apoptotic in a smaller proportion in the oSVZ than in the iSVZ of the premature ferret cortex.

3.2. EdU/BrdU-double labeled cells in cerebral gyral crowns and sulcal floors of 20-day-old ferrets

The density of EdU/ BrdU-double labeled cells was estimated in crowns of ten representative primary gyri from six cerebral hemispheres. The results are shown in Fig. 4E. In all gyral crowns, EdU/BrdU-double labeled cells were denser with upper cortical strata (Fig. 4A,B). More than half of EdU/BrdU-double labeled cells present throughout the entire cortical depth of each gyral crown was concentrated in the superficial portion of the outer stratum (Fig. 4E). Two groups of gyri were revealed by cluster analysis on the basis of diversity of EdU/BrdU-double labeled cell density: gyri with a relatively lower density, which convoluted in the primary motor and primary auditory cortices (i.e., posterior sigmoid gyrus, coronal gyrus (CNG), anterior ectosylvian gyrus, and posterior ectosylvian gyrus), and gyri with a relatively higher density, which convoluted in the prefrontal region (i.e., medial frontal cortex and anterior sigmoid gyrus (ASG)), cingulate region (i.e., cingulate gyrus), and parietooccipital region (i.e., lateral gyrus, suprasylvian gyrus, and visual cortical area) (Fig. 4D).

Next, the density of EdU/BrdU-double labeled cells was estimated in the floors of seven representative primary sulci from six cerebral hemispheres. The results are shown in Fig. 5D. In addition to gyral crowns, more than half of EdU/BrdU-double labeled cells present throughout the entire cortical depth of each sulcal floor was concentrated in the superficial portion of the outer stratum (Figs. 5A and B). Two groups of sulci were also revealed by cluster analysis based on the diversity of EdU/BrdU-double labeled cell density. Sulci in the primary motor and primary auditory cortices (i.e., coronal sulcus (cns) and rostral suprasylvian sulcus) and cingulate region (i.e., splenial sulcus) had a relatively lower density in their floor cortex. By contrast, sulci in the prefrontal region (i.e., cruciate sulcus and presylvian sulcus (prs)) and parietooccipital region (i.e., lateral sulcus and caudal suprasylvian sulcus) had a relatively higher density of EdU/BrdU-double labeled cells in their floor cortex (Fig. 5C).

3.3. EdU/BrdU-double staining with immunostaining for NeuN, PV, Olig2, and GFAP

To characterize the cell types of EdU/BrdU-double labeled cells, EdU/BrdU-double staining with immunostaining for NeuN, PV, Olig2,

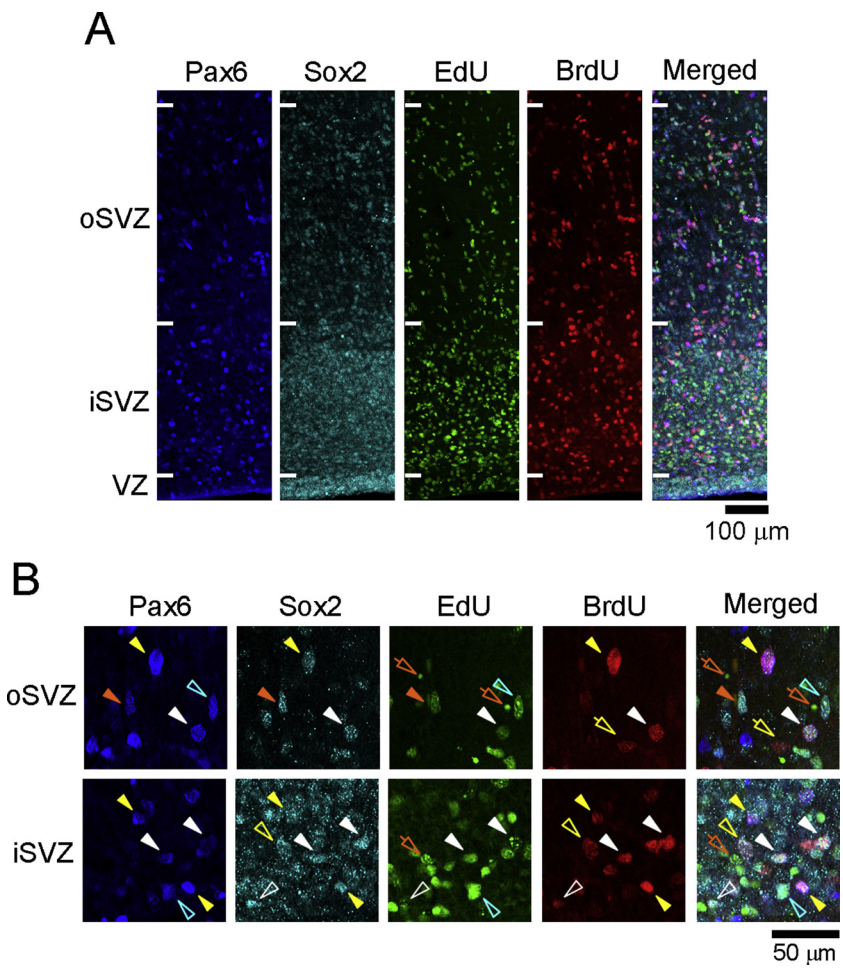

Fig. 1. Double immunofluorescence for Sox2 and Pax6 with EdU/BrdU-double labeling in the subventricular zone of the cerebral cortex of seven-day-old ferrets. (A) Low-magnification images of the outer and inner subventricular zones (oSVZ and iSVZ, respectively). (B) High-magnification images of the oSVZ and iSVZ. Ferret pups were given an EdU injection on postnatal day (PD) 5 followed by a BrdU injection on PD 7. The 48 h interval between EdU and BrdU injections covered the minimum times for the first and second S-phase of the self-renewing bRG. White open arrowheads: Sox2-positive/Pax6-negative progenitors with EdU/BrdU-double labeling; White closed arrowheads, Sox2-positive/Pax6-positive progenitors with EdU/BrdU-double labeling; Yellow open arrowheads, Sox2-positive/Pax6-negative progenitors with BrdU-single labeling; Yellow closed arrowheads, Sox2-positive/Pax6-positive progenitors with BrdU-single labeling; Yellow open arrows, BrdU-single labeled cells; Orange closed arrowheads, Sox2-positive/Pax6-positive progenitors with EdU-single labeling; Orange open arrows, EdU-single labeled cells; Light blue open arrowheads, Sox2-negative/Pax6-positive progenitors with EdU-single labeling.

Table 1
Densities of EdU- and/or BrdU-labeled cells and progenitors/cells immunostained for various markers in premature cortex of PD 7 ferrets.

	n =	Density (/mm^3)		
		iSVZ		oSVZ
EdU-single labeled cells	4	403,646 ± 33,170	-*-	114,475 ± 17,788
BrdU-single labeled cells	4	197,483 ± 4,060	-*-	83,550 ± 4,507
EdU/BrdU-double labeled cells	4	36,892 ± 7,279		28,754 ± 4,433
Sox2+ progenitors	4	1,265,191 ± 38,836	-*-	443,793 ± 17,788
Pax6+ progenitors	4	996,094 ± 16,438	-*-	481,771 ± 28,471
Olig2+ cells	4	375,977 ± 48,794		358,073 ± 25,735
cCP3+ cells	4	302,734 ± 46,636	-*-	87,891 ± 16,826

Data of the density were represented as mean ± SEM of 4 cerebral hemispheres.
"+" means "immunopositive."; * $P <$ 0.05 (non-parametric Scheffe's test); cCP, cleaved caspase 3.

Table 2
Percentages of Pax6-, Olig2-, or cCP3-labeling in Sox2-immunpositive progenitors of premature cortex in PD 7 ferrets.

	iSVZ			oSVZ	
Sox2+ progenitors					
Pax6+	22.1%	(161/728)	-*-	34.8%	(120/345)
Olig2+	12.4%	(111/894)	-*-	28.6%	(86/301)
cCP3+	15.2%	(149/980)		12.1%	(44/363)

Percentages were calculated by summing each immunolabeled cell counted within all ROIs from 4 cerebral hemispheres. The number of each labeled cell for calculating the percentages is shown in parentheses.
"+" means "immunopositive."; * $P <$ 0.01 (χ square test); cCP3, cleaved caspase 3.

and GFAP was carried out in the prefrontal cortex (i.e., ASG crown and prs floor) and primary motor cortex (i.e., CNG crown and cns floor), which contained higher and lower EdU/BrdU-double labeled cell densities defined by cluster analysis, respectively (ref. Figs. 4C and 5C). The density of EdU/BrdU-double labeled cells tended to be higher in the prefrontal cortex than in the primary motor cortex. The Friedman test revealed a region-related significant difference in density ($P <$ 0.05). Specifically, a significantly greater density was detected in the ASG crown compared to the CNG crown (Table 5). However, the cortical densities of EdU-single and BrdU-single cells did not differ among gyral and sulcal regions of prefrontal and primary motor cortices (Table 5).

Although EdU-single labeled cells were abundant in the iSVZ or oSVZ relative to BrdU-single labeled cells on PD 7, the density of EdU-single labeled cells in PD 20 cortex ranged from 0 (in the cns floor) to 868 ± 501/mm^3 (in the ASG crown), which was 1/100 or less than the BrdU-single labeled cell density (Table 5). This suggests that a great number of EdU-single labeled cells is lost during corticohistogenesis.

Neurons defined by NeuN immunostaining were densely packed throughout the entire cortical depth in both gyral crowns and sulcal floors (Figs. 4 and 5). The Friedman test revealed a region-related significant difference in neuron density ($P <$ 0.05). A statistically significant difference in neuron density was detected between CNS crowns and cns floors of the primary motor cortex (Table 5). Notably, 100% of EdU/BrdU-labeled cells were NeuN-positive in the gyral and sulcal regions examined (Table 6). Furthermore, GFAP and Olig2 immunostaining did not appear in EdU/BrdU-double labeled cells,

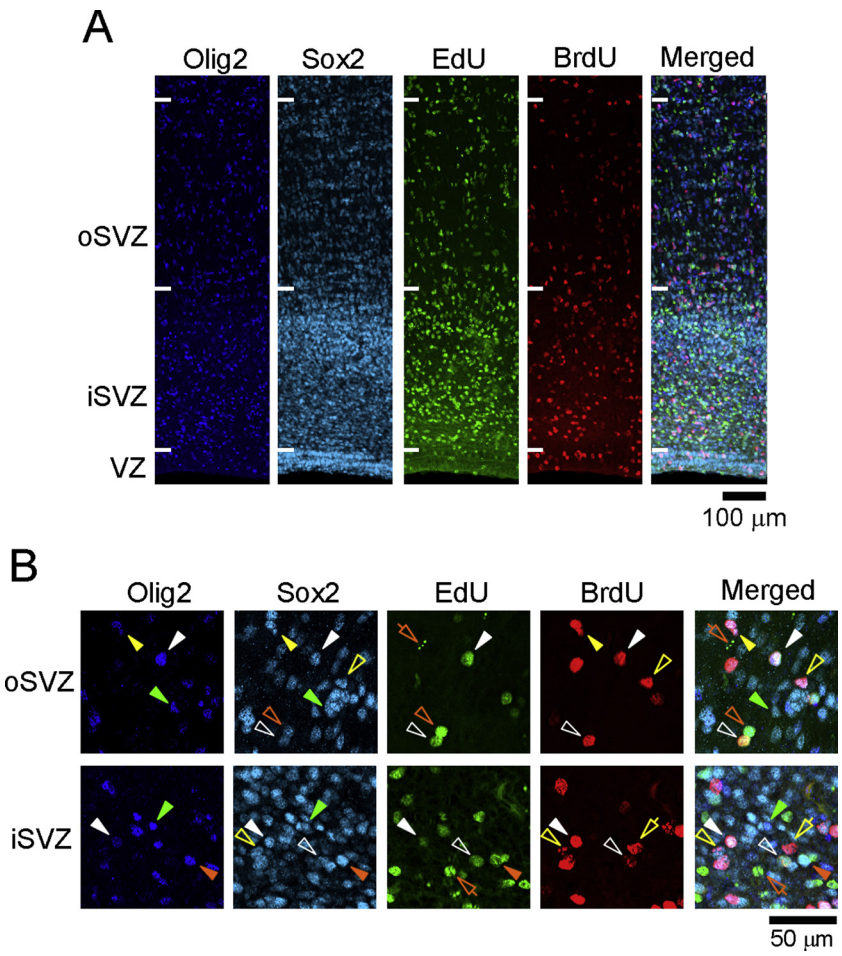

Fig. 2. Double immunofluorescence for Sox2 and Olig2 with EdU/BrdU-double labeling in the subventricular zone of the cerebral cortex of seven-day-old ferrets. (A) Low-magnification images of the outer and inner subventricular zones (oSVZ and iSVZ, respectively). (B) High-magnification images of the oSVZ and iSVZ. Ferret pups were given an EdU injection on postnatal day (PD) 5 followed by a BrdU injection on PD 7. The 48 h interval between EdU and BrdU injections covered the minimum times for the first and second S-phase of the self-renewing bRG. White open arrowheads, Sox2-positive/Olig2-negative progenitors with EdU/BrdU-double labeling; White closed arrowheads, Sox2-positive/Olig2-positive progenitors with EdU/BrdU-double labeling; Yellow open arrowheads, Sox2-positive/Olig2-negative progenitors with BrdU-single labeling; Yellow closed arrowheads, Sox2-positive/Olig2-positive progenitors with BrdU-single labeling; Yellow open arrows, BrdU-single labeled cells; Orange open arrows, EdU-single labeled cells; Orange open arrowheads, Sox2-positive/Olig2-negative progenitors with EdU-single labeling; Orange closed arrowheads, Sox2-positive/Olig2-positive progenitors with EdU-single labeling; Light green closed arrowheads, Sox2-positive/Olig2-postive progenitors without EdU and BrdU labeling.

Table 3
Percentages of labeling for various markers in EdU/BrdU-double labeled cells of premature cortex in PD 7 ferrets.

	iSVZ			oSVZ	
EdU/BrdU-double labeled cells					
Sox2+	85.3%	(58/68)		90.6%	(48/53)
Pax6+	83.9%	(26/31)		81.0%	(17/21)
Olig2+	33.3%	(7/21)		45.0%	(9/20)
cCP3+	56.3%	(9/16)	-*-	16.7%	(2/12)
EdU/BrdU-double labeled Sox2+ progenitors					
Pax6+	95.8%	(23/24)		84.2%	(16/19)
Olig2+	30.0%	(6/20)		47.4%	(9/19)
cCP3+	60.0%	(9/15)	-*-	20.0%	(2/10)

Percentages were calculated by summing each labeled cell counted within all ROIs from 4 cerebral hemispheres. The number of each labeled cell for calculating the percentages is shown in parentheses.
"+" means "immunopositive."; * $P < 0.05$ (χ square test); cCP3, cleaved caspase 3.

Table 4
Percentages of EdU and/or BrdU labeling in Sox2-positive/Pax6-positive and Sox2-positive/Olig2-positive progenitors of premature cortex in PD 7 ferrets.

	iSVZ			oSVZ	
Sox2+/Pax6+ progenitors					
no labeling	21.7%	(35/161)	-**-	36.7%	(44/120)
EdU-single labeling	18.6%	(30/161)		11.7%	(14/120)
BrdU-single labeling	45.3%	(73/161)		38.3%	(46/120)
EdU/BrdU-double labeling	14.3%	(23/161)		13.3%	(16/120)
Sox2+/Olig2+ progenitors					
no labeling	57.7%	(64/111)	-*-	43.0%	(37/86)
EdU-single labeling	15.3%	(17/111)		17.4%	(15/86)
BrdU-single labeling	21.6%	(24/111)		29.1%	(25/86)
EdU/BrdU-double labeling	5.4%	(6/111)		10.5%	(9/86)

Percentages were calculated by summing each labeled cell counted within all ROIs from 4 cerebral hemispheres. The number of each labeled cell for calculating the percentages is shown in parentheses.
"+" means "immunopositive."; * $P < 0.05$; ** $P < 0.01$ (non-parametric Scheffe's test).

although GFAP-positive astrocytes and Olig2-immunopositive oligodendrocytes were observed throughout the entire cortical depth in all gyral and sulcal regions examined (Table 5, Supplemental Fig. 3). Unexpectedly, only 6.7% of EdU/BrdU-labeled cells were Olig2-positive in the CNS (Table 6) when Olig2 immunostaining and NeuN immunostaining were performed independently. Nevertheless, cells with EdU/BrdU-double labeling in the PD 20 ferret cortex were defined as neurons.

PV immunostaining is known to appear transiently in non-pyramidal neurons of the developing ferret cortex (Gao et al., 2000). EdU and/or BrdU labeling were seen in PV-positive neurons distributed throughout the entire cortical depth of gyral and sulcal regions (Fig. 6). PV immunostaining was found in EdU/BrdU-labeled cells at a range from 62.5% (in the ASG crown) to 87.5% (in the cns floor) among the gyral and sulcal regions examined, although statistically significant regional variability was not detected (Table 6). Thus, EdU/BrdU-double labeling appeared mainly in PV-positive neurons.

3.4. EdU/BrdU-double staining with cCP3 immunostaining

To evaluate apoptotic loss of EdU/BrdU-double labeled cells during

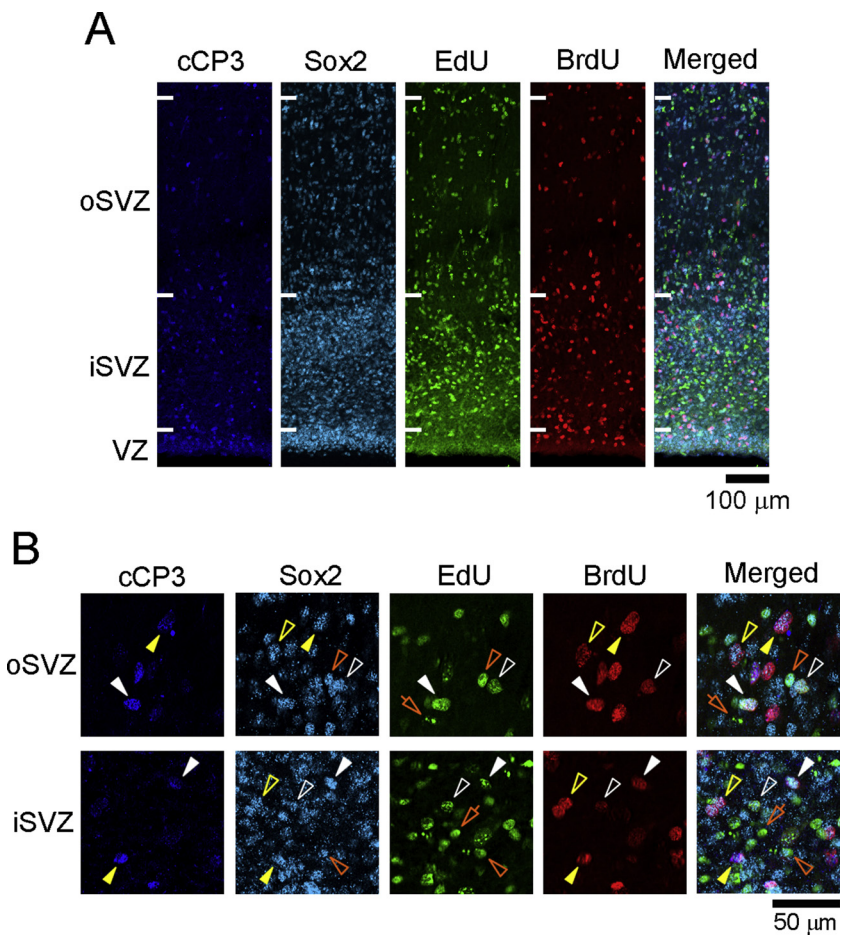

Fig. 3. Double immunofluorescence for Sox2 and cleaved caspase 3 (cCP3) with EdU/BrdU-double labeling in the subventricular zone of the cerebral cortex of seven-day-old ferrets. (A) Low-magnification images of the outer and inner subventricular zones (oSVZ and iSVZ, respectively). (B) High-magnification images of the oSVZ and iSVZ. Ferret pups were given an EdU injection on postnatal day (PD) 5 followed by a BrdU injection on PD 7. The 48 h interval between EdU and BrdU injections covered the minimum times for the first and second S-phase of the self-renewing bRG. White open arrowheads, Sox2-positive/cCP3-negative bRG with EdU/BrdU-double labeling; White closed arrowheads, Sox2-positive/cCP3-positive progenitors with EdU/BrdU-double labeling; Yellow open arrowheads, Sox2-positive/cCP3-negative progenitors with BrdU-single labeling; Yellow closed arrowheads, Sox2-positive/cCP3-positive progenitors with BrdU-single labeling; Orange open arrowheads, Sox2-positive/cCP3-negative progenitors with EdU-single labeling; Orange open arrows, EdU-single labeled cells.

corticohistogenesis, cCP3 immunostaining was carried out with EdU and BrdU labeling combined with PV immunostaining. cCP3 immunopositive cells were sparsely distributed throughout the entire cortical depth of gyral crowns and sulcal floors, and some of these cells were co-labeled with anti-PV (Fig. 6). cCP3-positive cells tended to be denser in the gyral and sulcal regions of the primary motor cortex than in the prefrontal cortex, although there were no statistically significant differences in the densities among the gyral and sulcal regions examined (Table 5). cCP3 immunostaining was seen in EdU/BrdU-double labeled cells with regional differences in the proportion, i.e., significantly lower in CNS crowns (0%) but higher in prs floors (15.0%) (Table 6). Since more than 60% of EdU/BrdU-double labeled cells exhibited PV immunostaining (Table 6), the proportion of cCP3 expression in EdU/BrdU-double labeled PV neurons was estimated. Although the proportion of cCP expression was 10% in the AGS and 0% in other regions, no statistically significant differences were detected among the gyral and sulcal regions examined (Table 6).

4. Discussion

It has been reported that cortical folding is enhanced by increasing the basal progenitor pool containing bRG in the oSVZ in the developing cerebral cortex via genetic manipulations of novel nuclear antigens such as Tmp1 and BAF170 (Stahl et al., 2013; Tuoc et al., 2013) and shh signaling in mice (Wang et al., 2016), and FGF8 and FGR receptors (Masuda et al., 2015; Matsumoto et al., 2017) and human-specific *ARHGAP11B* (Kalebic et al., 2018) in ferrets. A previous study using common marmoset fetuses revealed that oSVZ expansion preceded cortical folding (Sawada et al., 2014). These studies led me to suppose that the oSVZ bRG may be involved in gyrification during macroscale morphogenesis of the cerebral cortex. The design of EdU and BrdU injections successfully labeled Sox2-positive/Pax6-positive progenitors (defined as the bRG) at the late stage of cortical neurogenesis (Reillo and Borrell, 2012) and was used to track them during primary sulcogyrogenesis (Sawada and Watanabe, 2012; Sawada and Aoki, 2017). The labeled bRG may differentiate predominantly into neurons by PD 20, and more than 60% of neurons formed a population expressing PV during corticohistogenesis, as reported by Gao et al. (2000). However, their involvement in gyrification was unclear. The tracked neurons did not differ in density or the proportion of PV expression and apoptotic loss among gyral and sulcal regions. Further study is needed to clarify whether the density of PV neurons is altered in gyral and sulcal regions of animals with increased or decreased gyrification due to genetic manipulation.

Cortical layers II-III, also called the “outer stratum” or “supragranular layer,” are known to be mammal-specific and evolutionarily novel (Molnár et al., 2006) and their expansion is thought to have occurred in the process of mammalian evolution (Hutsler et al., 2005). In ferrets, the cerebral cortex expands continuously after PD 21 with progression of sulcal infolding in the prefrontal and cingulate regions and without progression of sulcal infolding in the parietooccipital regions (Sawada and Aoki, 2017). These regions were poorly myelinated in young adult ferrets (Sawada et al., 2013; Horiuchi-Hirose and Sawada, 2016). Cortical myelination is known to be sparse in multimodal association areas but heavy in unimodal areas (Burman and Rosa, 2009; Glasser et al., 2014). In humans and macaques, cortical expansion proceeds rapidly in cortical regions, which have slower maturation and greater cellular complexity, during postnatal development (Hill et al., 2010). Such postnatally-expanded regions correspond to cortical regions subject to human evolutionary expansion (Hill et al., 2010). Neurons derived from the bRG that undergo cell divisions at PDs 5 and 7 were found to exist at higher densities in gyral crowns and

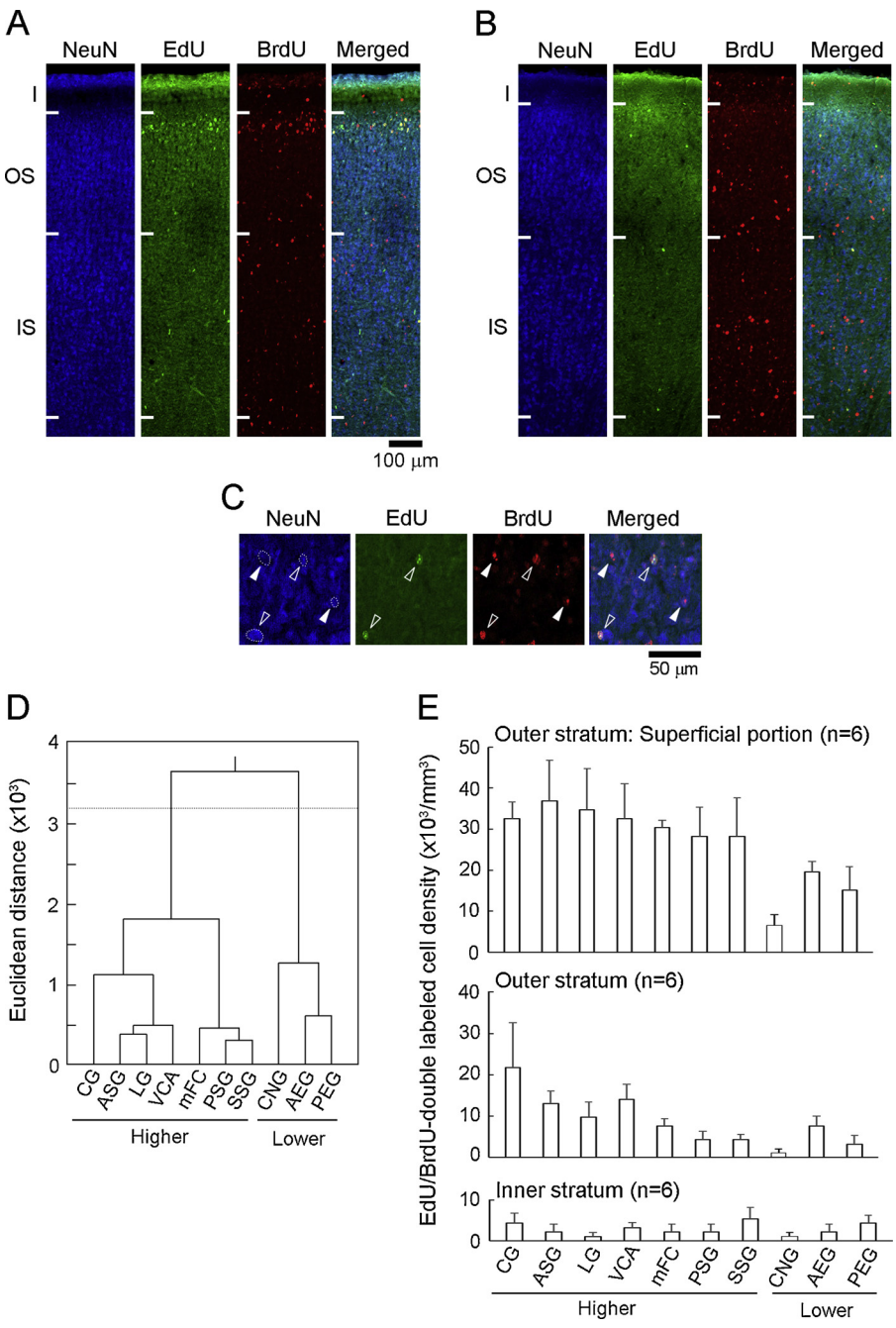

Fig. 4. Immunofluorescence for NeuN with EdU/BrdU-double labeling in the gyral crowns of the cerebral cortex of 20-day-old ferrets. (A) Low-magnification images of the cortical depth in the crown of the anterior sigmoid gyrus. (B) Low-magnification images of the entire cortical depth in the crown of the central gyrus. The anterior sigmoid gyrus and central gyrus were selected as representative gyri that contained relatively higher and lower densities of EdU/BrdU-double labeled cells, respectively. (C) High-magnification images of the superficial portion of the outer stratum. Dotted circles surround the NeuN-stained profiles, which were stained for EdU and/or BrdU. Open arrowheads, EdU/BrdU-double labeled neurons; Closed arrowheads, BrdU-single labeled neurons. (D) A dendrogram showing two groups of gyral regions clustered by the diversity of the cortical density of EdU/BrdU-double labeled neurons. Higher, density group of gyral regions; Lower density group of gyral regions. (E) Bar graphs of EdU/BrdU-double labeled cell density in the superficial and underlying portions of the outer and inner strata. Ferret pups were given an EdU injection on postnatal day (PD) 5 followed by a BrdU injection on PD 7. The 48 h interval between EdU and BrdU injections covered the minimum times for the first and second S-phase of the self-renewing bRG. I, layer I; AEG, anterior ectosylvian gyrus; ASG, anterior sigmoid gyrus; CG, cingulate gyrus; IS, inner stratum (corresponding to layers IV—VI); LG, lateral gyrus; mFC, medial frontal cortex; OS, outer strata (corresponding to layers II-III); PEG, posterior ectosylvian gyrus; PSG, posterior sigmoid gyrus; SSG, suprasylvian gyrus; VCA, visual cortical area.

sulcal floors of the prefrontal, cingulate and/or, parietooccipital cortices in ferrets. Therefore, the bRG at late cortical neurogenesis may be implicated in the evolution of cortical expansion in ferrets. The results of this study may support a hypothesis by Nonaka-Kinoshita et al. (2013) that the bRG is one of the factors responsible for evolutionary expansion.

The relationship between cortical expansion and sulcal infolding differed depending on the developmental stage. In a study using macaques, cortical expansion was first correlated with sulcogyrogenesis and subsequently with generating secondary sulci and deepening primary sulci in cortical regions associated with evolutionary expansion (Sawada et al., 2012, 2017). On the other hand, the bRG was abundant in the oSVZ of the developing cortex of marmosets, which have a poorly gyrencephalic cerebrum (Hevner and Haydar, 2012; Kelava et al., 2012). Continuous expansion of the cortex, but reduced gyrification, was observed in marmosets after birth (Sawada et al., 2014). Thus, bRG-related evolutionary cortical expansion may be secondary to sulcal development, although it is certainly a factor influencing gyrification during macroscale morphogenesis of the cerebral cortex. The striking species-specific patterns of gyrification may be primarily due to interactions of bRG-related evolutionary expansion with other factors, such as a tension from subcortical white matter (Van Essen, 1997; Hilgetag and Barbas, 2006; Herculano-Houzel et al., 2010; Sawada et al., 2012). This supposition would be supported by tracking bRG-derived neurons in poorly gyrencephalic animals such as marmosets, or disturbing subcortical white matter development in gyrencephalic animals, such as ferrets and macaque monkeys, during corticohistogenesis.

EdU-single labeled cells were particularly abundant in the iSVZ of the PD 7 premature cortex, but sparse throughout the PD 20 cortex in ferrets. It is unclear whether EdU and/or BrdU caused apoptosis of the bRG, IPC, and the neurons derived from them. A few pyknotic cells were reportedly induced in the developing neocortex of fetal rats by

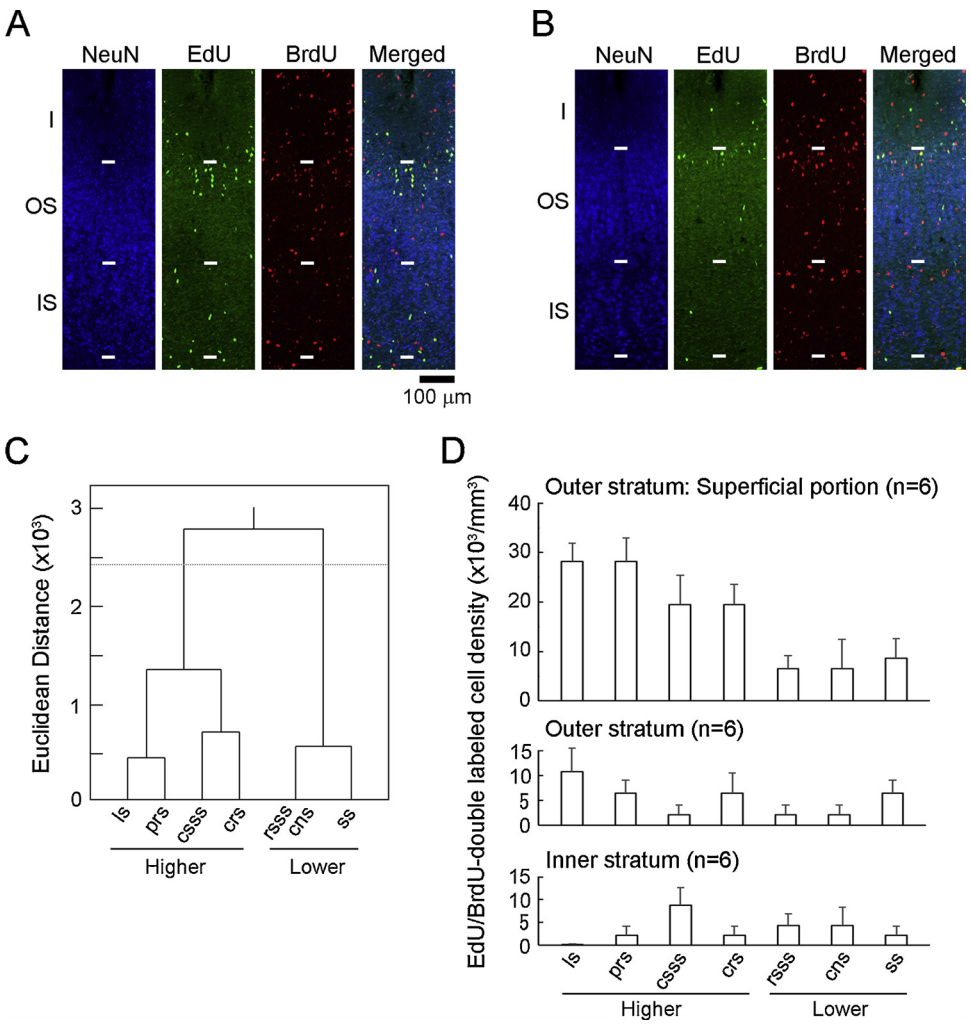

Fig. 5. Immunofluorescence for NeuN with EdU/BrdU-double labeling in sulcal floors of the cerebral cortex of 20-day-old ferrets. (A) Low-magnification images of the entire cortical depth in the floor of the presylvian sulcus. (B) Low-magnification images of the entire cortical depth in the floor of the central sulcus. The presylvian sulcus and central sulcus were selected as representative sulci that contained relatively higher and lower densities of EdU/BrdU-double labeled cells, respectively. (C) A dendrogram showing two groups of sulcal regions clustered by the diversity of the cortical density of EdU/BrdU-double labeled neurons. Higher, density group of sulcal regions; Lower density group of sulcal regions. (E) Bar graphs of EdU/BrdU-double labeled cell density in the superficial and underlying portions of the outer and inner strata. Ferret pups were given an EdU injection on postnatal day (PD) 5 followed by a BrdU injection on PD 7. The 48 h interval between EdU and BrdU injections covered the minimum times for the first and second S-phase of the self-renewing bRG. I, layer I; crs, cruciate sulcus; cns, central sulcus; csss, caudal suprasylvian sulcus; IS, inner stratum (corresponding to layers IV–VI); LG, lateral sulcus; OS, outer strata (corresponding to layers II-III); rsss, rostral suprasylvian sulcus; ss, splenial sulcus.

Table 5
Densities of EdU- and/or BrdU-labeled cells and cells immunostained for various markers in the entire cortical depth of representative primary gyral and sulcal regions in PD 20 ferrets.

	n=	Gyral crowns		Sulcal floors	
		ASG	CNG	prs	cns
EdU-single labeled cells	6	868 ± 501	434 ± 396	723 ± 660	0
BrdU-single labeled cells	6	142,361 ± 27,317	120,660 ± 21,251	138,166 ± 37,061	81,742 ± 12,957
EdU/BrdU-double labeled cells	6	13,455 ± 1,135	* 2,170 ± 731	12,297 ± 2,381	4,340 ± 2,506
NeuN+ cells	6	580,295 ± 21,017	658,420 ± 37,754	* 621,528 ± 53,326	391,059 ± 35,236
PV+ cells	6	19,531 ± 2,928	16,927 ± 2,013	20,978 ± 281	24,595 ± 4,176
Olig2+ cells	6	58,160 ± 4,193	56,424 ± 4,974	52,083 ± 10,778	45,573 ± 3,929
GFAP+ cells	6	3,472 ± 1,175	1,302 ± 532	2,170 ± 1,981	2,170 ± 1,353
cCP3+ cells	6	3,308 ± 1,555	19,965 ± 7,228	7,957 ± 1,218	11,574 ± 7,633
PV+/ cCP3+	6	868 ± 501	4,774 ± 2,074	723 ± 660	2,170 ± 1,353

Data of the density were represented as mean ± SEM of 6 cerebral hemispheres.
"+" means "immunopositive."; * $P < 0.05$ (non-parametric Scheffe's test); cCP3, cleaved caspase 3; PV. Parvalbumin.

administering BrdU at a dose of 50 μg/g body weight for 6 days (gestational days 9.5 through 15.5) (Ogawa et al., 2005). Accumulation of excess BrdU in neuronal stem/progenitor cells may have slightly neurotoxic effects on the developing cortex. However, the doses of EdU and BrdU used here (30 μg/g body weight) were equal to or less than those used in previous studies involving ferret pups (Borrell et al., 2006; Turrero García et al., 2016) and are not considered to cause loss of EdU-single labeled cells in the ferret cortex by PD 20. Further study is needed to identify the types of SVZ progenitors of EdU-single labeled cells in the PD 7 cortex and to clarify the reason why EdU-single labeled cell are lost during corticohistogenesis by tracking them in ferrets.

The present study was able to track bRG-derived neurons, defined

Table 6
Percentages of expression of various markers in EdU/BrdU-double labeled cells in the entire cortical depth of representative primary gyral and sulcal regions of PD 20 ferrets.

	Gyral crowns				Sulcal floors			
	ASG		CNG		prs		cns	
EdU/BrdU-double labeled cells								
NeuN +	100.0%	(10/10)	100.0%	(10/10)	100.0%	(14/14)	100.0%	(4/4)
PV +	62.5%	(10/16)	77.8%	(7/9)	60.0%	(12/20)	87.5%	(7/8)
GFAP +	0%	(0/25)	0%	(0/13)	0%	(0/9)	0%	(0/5)
Olig2 +	0%	(0/22)	6.7%	(1/15)	0%	(0/31)	0%	(0/14)
cCP 3 +	6.3%	(1/16)	0%	(0/46)$^{\#}$	15.0%	(3/20)*	12.5%	(1/8)
EdU/BrdU-double labeled PV neurons								
cCP3 +	10.0%	(1/10)*	0%	(0/7)	0%	(0/12)	0%	(0/7)

Percentages were calculated by summing each labeled cell counted within all ROIs from 6 cerebral hemispheres. The number of each labeled cell for calculating the percentages is shown in parentheses.
" + " means "immunopositive."; * $P < 0.05$, ** $P < 0.01$, significantly higher than other regions (χ square test); $^{\#}$ $P < 0.05$, $^{\#\#}$ $P < 0.01$, significantly lower than other regions (χ square test); cCP3, cleaved caspase 3; PV. parvalbumin.

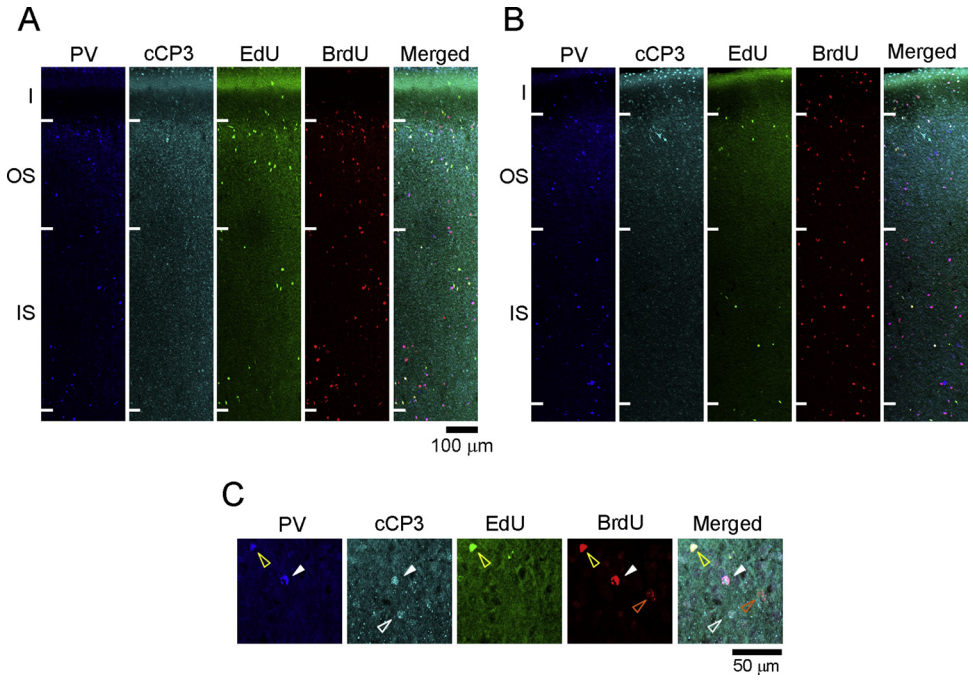

Fig. 6. Double immunofluorescence for parvalbumin (PV) and cleaved caspase 3 (cCP3) with EdU/BrdU-double labeling in gyral crowns of the cerebral cortex of 20-day-old ferrets. (A) A low-magnification image of the entire cortical depth of the crown of the anterior sigmoid gyrus. (B) A low-magnification image of the entire cortical depth of the crown of central gyrus. The anterior sigmoid gyrus and central gyrus were selected as representative gyri that contained relatively higher and lower densities of EdU/BrdU-double labeled cells, respectively. (C). High-magnification images of the inner stratum. Ferret pups were given an EdU injection on postnatal day (PD) 5 followed by a BrdU injection on PD 7. The 48 h interval between EdU and BrdU injections covered the minimum times for the first and second S-phase of the self-renewing bRG. White open arrowheads, PV-negative/cCP3-positive cells without EdU and BrdU labeling; White closed arrowheads, PV-positive/cCP3-positive neurons with BrdU-single labeling; Yellow open arrowheads, PV-positive/cCP3-negative neurons with EdU/BrdU-double labeling; Orange open arrowheads, PV-negative/cCP3-negative cells with BrdU-single labeling. I, layer I; IS, inner stratum (corresponding to layers IV-VI), LG, lateral sulcus; OS, outer strata (corresponding to layers II-III).

by the S-shape duration and transcription factor expression, during a course of primary sulcogyrogenesis in ferrets. Although neurons generated within a narrow time window of cortical neurogenesis were tracked, notable findings were obtained, including the expression of PV during corticohistogenesis and the involvement of their distributional diversity in evolutionary cortical expansion. Combined with findings from previous investigations using marmosets (Hevner and Haydar, 2012; Kelava et al., 2012; Sawada et al., 2014), bRG-related evolutionary cortical expansion may have contributed secondarily to sulcal development. These findings are advantageous for understanding gyrification mechanisms during macroscale morphogenesis of the cerebral cortex at the cellular level.

Conflict of interest

There are no conflicts of interest.

Acknowledgments

The authors wish to thank Mr. Masahito Nagata (Faculty of Animal Breeding, Nakaizu Laboratory, SLC) and Ms. Shiori Kamiya (The Department of Nutrition, Faculty of Medical and Health Sciences, Tsukuba International University) for their technical assistances. This work was supported by JSPS KAKENHI (15K08144).

References

Borrell, V., 2018. How cells fold the cerebral cortex. J. Neurosci. 38, 776–783.
Borrell, V., Kaspar, B.K., Gage, F.H., Callaway, E.M., 2006. In vivo evidence for radial migration of neurons by long-distance somal translocation in the developing ferret visual cortex. Cereb. Cortex 16, 1571–1583.
Burman, K.J., Rosa, M.G., 2009. Architectural subdivisions of medial and orbital frontal cortices in the marmoset monkey (*Callithrix jacchus*). J. Comp. Neurol. 514, 11–29.
Di Curzio, D.L., Buist, R.J., Del Bigo, M.R., 2013. Reduced subventricular zone proliferation and white matter damage in juvenile ferrets with kalion-induced hydrocephalus. Exp. Neurol. 248, 112–128.
Fietz, S.A., Kelava, I., Vogt, J., Wilsch-Bräuninger, M., Stenzel, D., Fish, J.L., Corbeil, D.,

Riehn, A., Distler, W., Nitsch, R., Huttner, W.B., 2010. OSVZ progenitors of human and ferret neocortex are epithelial-like and expand by integrin signaling. Nat. Neurosci. 13, 690–699.
Fukui, Y., Bedi, K.S., 2000. Application of stereology to the central nervous system: estimation of numerical densities of cells and synapses or cell number. Congenit. Anom. (Kyoto) 40, 1–7.
Gao, W.J., Wormington, A.B., Newman, D.E., Pallas, S.L., 2000. Development of inhibitory circuitry in visual and auditory cortex of postnatal ferrets: immunocytochemical localization of calbindin- and parvalbumin-containing neurons. J. Comp. Neurol. 422, 140–157.
Gertz, C.C., Lui, J.H., LaMonica, B.E., Wang, X., Kriegstein, A.R., 2014. Diverse behaviors of outer radial glia in developing ferret and human cortex. J. Neurosci. 34 2559–2270.
Glasser, M.F., Goyal, M.S., Preuss, T.M., Raichle, M.E., Van Essen, D.C., 2014. Trends and properties of human cerebral cortex: correlations with cortical myelin content. Neuroimage 93, 165–175.
Gundersen, H.J.G., 1977. Notes on the estimation of the numerical density of arbitrary profiles: the edge effect. J. Microsc. 111, 219–223.
Hansen, D.V., Lui, J.H., Parker, P.R.L., Kriegstein, A.R., 2010. Neurogenic radial glia in the outer subventricular zone of human neocortex. Nature 464, 554–561.
Herculano-Houzel, S., Mota, B., Wong, P., Kaas, J.H., 2010. Connectivity-driven white matter scaling and folding in primate cerebral cortex. Proc. Natl. Acad. Sci. U.S.A. 107, 19008–19013.
Hevner, R.F., Haydar, T.F., 2012. The (not necessarily) convoluted role of basal radial glia in cortical neurogenesis. Cereb. Cortex 22, 465–468.
Hilgetag, C.C., Barbas, H., 2006. Role of mechanical factors in the morphology of the primate cerebral cortex. PLoS Comput. Biol. 2, e22.
Hill, J., Inder, T., Neil, J., Dierker, D., Harwell, J., Van Essen, D., 2010. Similar patterns of cortical expansion during human development and evolution. Proc. Natl. Acad. Sci. U.S.A. 107, 13135–13140.
Horiuchi-Hirose, M., Sawada, K., 2016. Differential cortical laminar structure revealed by NeuN immunostaining and myeloarchitecture between sulcal and gyral regions independent of sexual dimorphisms in the ferret cerebrum. Anat. Rec. Hoboken (Hoboken) 299, 1003–1011.
Hutsler, J.J., Lee, D.G., Porter, K.K., 2005. Comparative analysis of cortical layering and supragranular layer enlargement in rodent carnivore and primate species. Brain Res. 1052, 71–81.
Kalebic, N., Gilardi, C., Albert, M., Namba, T., Long, K.R., Kostic, M., Langen, B., Huttner, W.B., 2018. Human-specific *ARHGAP11B* induces hallmarks of neocortical expansion in developing ferret neocortex. Elife 7, e41241.
Kawasaki, H., Toda, T., Tanno, K., 2013. In vivo genetic manipulation of cortical progenitors in gyrencephalic carnivores using in utero electroporation. Biol. Open 15, 95–100.
Kelava, I., Reillo, I., Murayama, A.Y., Kalinka, A.T., Stenzel, D., Tomancak, P., Matsuzaki, F., Lebrand, C., Sasaki, E., Schwamborn, J.C., Okano, H., Huttner, W.B., Borrell, V., 2012. Abundant occurrence of basal radial glia in the subventricular zone of embryonic neocortex of a lissencephalic primate, the common marmoset Callithrix jacchus. Cereb. Cortex 22, 469–481.
Kroenke, C.D., Bayly, P.V., 2018. How forces fold the cerebral cortex. J. Neurosci. 38, 767–775.
Lewitus, E., Kelava, I., Huttner, W.B., 2013. Conical expansion of the outer subventricular zone and the role of neocortical folding in evolution and development. Front. Hum. Neurosci. 7, 24.
Lui, J.H., Hansen, D.V., Kriegstein, A.R., 2011. Development and evolution of the human neocortex. Cell 146, 18–36.
Martínez-Cerdeño, V., Cunningham, C.L., Camacho, J., Antczak, J.L., Prakash, A.N., Cziep, M.E., Walker, A.I., Noctor, S.C., 2012. Comparative analysis of the subventricular zone in rat, ferret and macaque: evidence for an outer subventricular zone in rodents. PLoS One 7, e30178.
Masuda, K., Toda, T., Shinmyo, Y., Ebisu, H., Hoshiba, Y., Wakimoto, M., Ichikawa, Y., Kawasaki, H., 2015. Pathophysiological analyses of cortical malformation using gyrencephalic mammals. Sci. Rep. 5, 15370.
Matsumoto, N., Shinmyo, Y., Ichikawa, Y., Kawasaki, H., 2017. Gyrification of the cerebral cortex requires FGF signaling in the mammalian brain. Elife 6 pii, e29285.
Molnár, Z., Métin, C., Stoykova, A., Tarabykin, V., Price, D.J., Francis, F., Meyer, G., Dehay, C., Kennedy, H., 2006. Comparative aspects of cerebral cortical development. Eur. J. Neurosci. 23, 921–934.
Nonaka-Kinoshita, M., Reillo, I., Artegiani, B., Martínez-Martínez, M.Á., Nelson, M., Borrell, V., Calegari, F., 2013. Regulation of cerebral cortex size and folding by expansion of basal progenitors. EMBO J. 32, 1817–1828.
Ogawa, T., Kuwagata, M., Muneoka, K.T., Shioda, S., 2005. Neuropathological examination of fetal rat brain in the 5-bromo-2′-deoxyuridine-induced neurodevelopmental disorder model. Congenit. Anom. (Kyoto) 45, 14–20.
Poluch, S., Jablonska, B., Juliano, S.L., 2008. Alteration of interneuron migration in a ferret model of cortical dysplasia. Cereb. Cortex 18, 78–92.
Reillo, I., Borrell, V., 2012. Germinal zones in the developing cerebral cortex of ferret: ontogeny, cell cycle kinetics, and diversity of progenitors. Cereb. Cortex 22, 2039–2054.
Reillo, I., de Juan Romero, C., García-Cabezas, M.Á., Borrell, V., 2011. A role for intermediate radial glia in the tangential expansion of the mammalian cerebral cortex. Cereb. Cortex 21, 1674–1694.
Saliu, A., Adise, S., Xian, S., Kudelska, K., Rodríguez-Contreras, A., 2014. Natural and lesion-induced decrease in cell proliferation in the medial nucleus of the trapezoid body during hearing development. J. Comp. Neurol. 522, 971–985.
Sawada, K., Aoki, I., 2017. Biphasic aspect of sexually dimorphic ontogenetic trajectory of gyrification in the ferret cerebral cortex. Neuroscience 364, 71–81.
Sawada, K., Fukunishi, K., Kashima, M., Imai, N., Saito, S., Aoki, I., Fukui, Y., 2017. Regional difference in sulcal infolding progression correlated with cerebral cortical expansion in cynomolgus monkey fetuses. Congenit. Anom. (Kyoto) 57, 114–117.
Sawada, K., Fukunishi, K., Kashima, M., Saito, S., Sakata-Haga, H., Aoki, I., Fukui, Y., 2012. Fetal gyrification in cynomolgus monkeys: a concept of developmental stages of gyrification. Anat. Rec. Hoboken (Hoboken) 295, 1065–1074.
Sawada, K., Hikishima, K., Murayama, A.Y., Okano, H.J., Sasaki, E., Okano, H., 2014. Fetal sulcation and gyrification in common marmosets (*Callithrix jacchus*) obtained by *ex vivo* magnetic resonance imaging. Neuroscience 25, 158–174.
Sawada, K., Horiuchi-Hirose, M., Saito, S., Aoki, I., 2013. MRI-based morphometric characterizations of sexual dimorphism of the cerebrum of ferrets (*Mustela putorius*). Neuroimage 83, 294–306.
Sawada, K., Horiuchi-Hirose, M., Saito, S., Aoki, I., 2015. Sexual dimorphism of sulcal morphology of the ferret cerebrum revealed by MRI-based sulcal surface morphometry. Front. Neuroanat. 9, 55.
Sawada, K., Watanabe, M., 2012. Development of cerebral sulci and gyri in ferrets (*Mustela putorius*). Congenit. Anom. (Kyoto) 52, 168–175.
Shitamukai, A., Konno, D., Matsuzaki, F., 2011. Oblique radial glial divisions in the developing mouse neocortex induce self-renewing progenitors outside the germinal zone that resemble primate outer subventricular zone progenitors. J. Neurosci. 31, 3683–3695.
Stahl, R., Walcher, T., De Juan Romero, C., Pilz, G.A., Cappello, S., Irmler, M., Sanz-Aquela, J.M., Beckers, J., Blum, R., Borrell, V., Götz, M., 2013. Trnp1 regulates expansion and folding of the mammalian cerebral cortex by control of radial glial fate. Cell 153, 535–549.
Sterio, D.C., 1984. The unbiased estimation of number and sizes of arbitrary particles using the disector. J. Microsc. 134, 127–136.
Tuoc, T.C., Boretius, S., Sansom, S.N., Pitulescu, M.E., Frahm, J., Livesey, F.J., Stoykova, A., 2013. Chromatin regulation by BAF170 controls cerebral cortical size and thickness. Dev. Cell 25, 256–269.
Turrero García, M., Chang, Y., Arai, Y., Huttner, W.B., 2016. S-phase duration is the main target of cell cycle regulation in neural progenitors of developing ferret neocortex. J. Comp. Neurol. 524, 456–470.
Van Essen, D.C., 1997. A tension-based theory of morphogenesis and compact wiring in the central nervous system. Nature 385, 313–318.
Wang, L., Hou, S., Han, Y.G., 2016. Hedgehog signaling promotes basal progenitor expansion and the growth and folding of the neocortex. Nat. Neurosci. 19, 888–896.
Wang, X., Tsai, J.W., LaMonica, B., Kriegstein, A.R., 2011. A new subtype of progenitor cell in the mouse embryonic neocortex. Nat. Neurosci. 14, 555–561.